

Quantitative Feedback Theory design of valve position control for co-ordinated superheater control of main steam temperatures of power plant boilers

Cheriska Polton* and Edward Boje**

Department of Electrical Engineering, University of Cape Town, Cape Town, South Africa, 7700

**(e-mail: cheriskal8@gmail.com)*

*** (e-mail: edward.boje@uct.ac.za)*

Abstract: This paper presents an application of a Single-Input Single-Output (SISO) controller and a Valve Position Controller (VPC) using robust Proportional-Integral (PI) controllers designed using Quantitative Feedback Theory (QFT) specifications to control superheater outlet steam temperatures of a 600MW once-through boiler. To illustrate the methodology, a dynamic model of a tower-type boiler was modelled using Flownex® to test the VPC design application with structured uncertainty under varying load and disturbance conditions. The results show that the valve position controller application is more efficient than the SISO technique, allowing the final attemperator more bandwidth to deal with unexpected temperature changes.

Keywords: System Identification, robust feedback control, quantitative feedback theory, valve position control, superheater attemperation, PI controller.

1. INTRODUCTION

One of the most critical variables in a coal fired boiler is the main or outlet steam temperature as errors in this can cause extensive damage to the turbine blades and boiler tubes. Although high steam temperature is beneficial for thermal efficiency, it accelerates creep damage and thermal fatigue in high temperature components which is detrimental to the life of these components. Alternatively, low steam temperatures increase the moisture content in the last stages of the turbine which causes the turbine blades to erode and eventually to fail. Main steam temperatures are controlled by maintaining a balance between heat input (flue gas), and feedwater and spray water flowrates. Shinsky (2006) defines a cascade controller as a multi-loop structure where the output of the primary or outer loop controller generates a setpoint for the secondary or inner loop controller. Molbak and Mortensen (2003) used a single-input single-output (SISO) proportional and integral (PI) cascade controller where any disturbance negatively affecting the inner loop of the controller is corrected before it has any influence on the primary outer loop due to the faster dynamics of the inner loop. Sanchez, Arroyo and Villavicencio (2003) designed and simulated a multivariable predictive controller to control the steam temperature of a fossil fuel power plant. Spliethoff (1986) used a state controller for controlling the main steam outlet temperature for a once through boiler.

This paper proposes a design methodology for a PI controller using Quantitative Feedback Theory (QFT) in MATLAB® to compare the application of a SISO control technique and a Valve Position Controller (VPC) under uncertain parameter variations. The design method applies to convection pass heat exchangers and aims to minimise the control effort of the attemperation valves while allowing robust control of the main

steam temperatures. This controller was designed for and tested at 100%, 97% and 70% MCR (Maximum Continuous Rating) operating load conditions. Designing a robust controller to meet the design steam conditions at the turbine inlet helps protect thick wall components against long term overheating and thermal stress and improves efficiency while maintaining long term plant health.

A simplified three-stage superheater (SH) convection pass of a Benson boiler was modelled in Flownex® with attemperation control around SH2 and SH3 stages using fundamental energy and mass balances. This model was used to simulate plant data while being subjected to variable heat inputs and load disturbances.

2. CONVECTION PASS

This section of the paper details the modelling of the convection pass of a once-through Benson type boiler. Figure 1 illustrates the configuration and flow path of the three superheaters and two reheaters of the convection pass. Steam, which is generated in the furnace enters the convection pass at SH1, which is a platen superheater and is located in the radiant zone of the boiler with large and variable heat uptake and exits at SH3. Flue gas flows from the furnace, through the convection pass towards the roof of the boiler, resulting in cross-counter flow heat exchanger in respect to the steam.

The steam outlet temperature is controlled by an attemperation device which injects atomised feedwater through Attemperators 1, 2 and 3, although Attemperator 1 temperature control valve serves as a safety circuit for large temperature increases and is generally not in control during normal operating conditions.

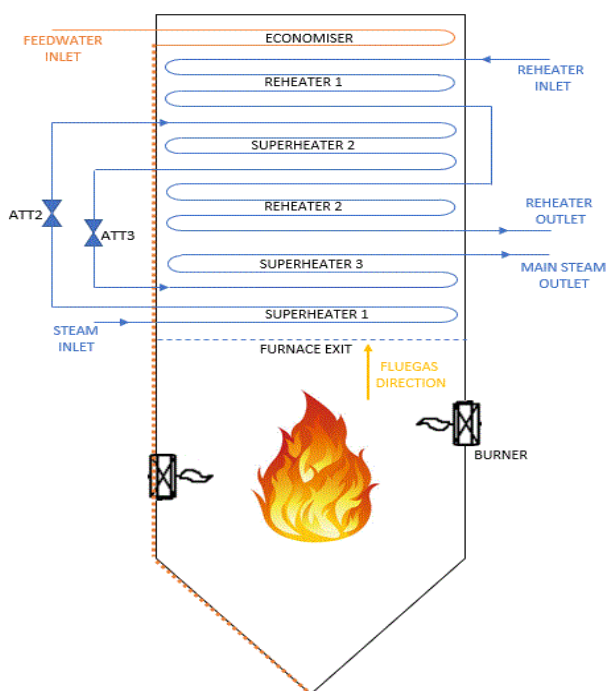


Figure 1: A simplified Benson boiler component configuration

2.1. Maximum Continuous Rating (MCR)

For this boiler configuration, 100% of Maximum Continuous Rating (MCR) is equivalent to 600 MW load demand, requiring steam conditions of 540 °C at 16.6 MPa. The MCR is the capacity of the boiler to generate and continuously supply a guaranteed steam mass flow according to specific pressure and temperature conditions and fuels, with no shortfalls (such as tube overheating).

2.2. Flownex® thermofluid model

Flownex®, a thermofluid simulation package, was used to develop a dynamic thermofluid process model of the convection pass. For simplicity, the physical properties of the convection pass were integrated into a series of lumped, single flow (i.e. assuming common conditions in all parallel tubes) heat exchangers. Although the control of reheat steam is beyond the scope of this paper, the second reheater stage was included to model the relevant flue gas temperatures in the boiler. Heat transfer from the flue gas further heats the steam through convection (predominantly), conduction and radiation in the convection pass to meet final steam conditions before entering the turbine.

2.2.1. External Convection

Convection refers to the transfer of heat between a solid surface and a fluid moving over the surface. Total heat transfer from flue gas to the external tube surface achieved via external convection and gas radiation. The Nusselt number (Nu) was calculated using the Zukauskus correlation using the Reynolds number (Re), Prandtl number (Pr), $c = 0.27$, $m = 0.63$ and

$n = 0.36$ (Schlunder, 1983), and the subscript s represents the specific property evaluated at surface temperature.

$$Nu = c \cdot Re^m \cdot Pr^n \cdot \left(\frac{Pr}{Pr_s} \right)^{1/4} \quad (1)$$

The flue gas volume is cooled due to the loss of the heat energy transferred to the superheater tube walls. The total external heat transfer coefficient is calculated as the summation of the convective and gas radiative heat transfer coefficients.

$$h_{combined} = h_{conv.ext} + h_{radiation} \quad (2)$$

2.2.2. Conduction

Heat transfer between the external tube surface and internal tube surface is via conduction. According to Fourier's Law, the transient conductive heat transfer equation is:

$$q_x = -kA \frac{dT}{dx} = -kA \frac{T_o - T_i}{x} \quad (3)$$

where the amount of heat transfer depends on the thermal conductivity of the material k , the thickness of the material x , the surface area of the tube A and the difference in temperature between the two surfaces. To approximate the effect of fouling, the overall heat transfer coefficient can be adjusted for clean tubes with a coefficient of effectiveness ($\psi_{fouling}$) of 0.65 (Zhang, et al., 2016).

2.2.3. Internal Convection

Total heat transfer between the internal tube surface and steam is via internal convection. The Nusselt number for turbulent flow was calculated using the Dittus Boelter correlation where $n = 0.4$ for heating (Schlunder, 1983):

$$Nu = 0.023 \cdot Re^{0.8} \cdot Pr^n \quad (4)$$

The forced convection heat transfer coefficient is calculated using the following relation where $\lambda_{fluid} [W/mK]$ is the fluid's thermal conductivity evaluated at the mean temperature of the control volume and $d_e [m]$ is the hydraulic diameter of the tube.

$$h_{conv} = \frac{Nu_{conv} \cdot \lambda_{fluid}}{d_e} \quad (5)$$

Typical values for the flue gas to wall surface and wall surface to steam for 100% MCR were calculated as follows:

Table 1: Typical values for flue gas and steam parameters

	Wall surface to steam		Flue gas to wall surface	
	Nu	$h [W/m^2K]$	Nu	$h [W/m^2K]$
SH2	1487	4164.9	28.4	71.5
SH3	1589.1	4562.9	25.0	101.3
SH1	6449.8	16685.2	26.1	114.2

The overall heat transfer coefficient is:

$$U = \frac{\Psi_{fouling}}{h_{combined} + h_{steam}} \quad (6)$$

Using Newton's Law of cooling, the heat uptake (Q) is calculated using the overall convective heat transfer coefficient, the surface area (A) exposed and the logarithmic mean temperature difference (T_{LMTD}) between the inlet and outlet of the heat exchanger.

$$Q = U \cdot A \cdot (T_{LMTD}) \quad (7)$$

Figure 2 summarises the methodology used to model the convection and radiation heat transfer components in Flownex®.

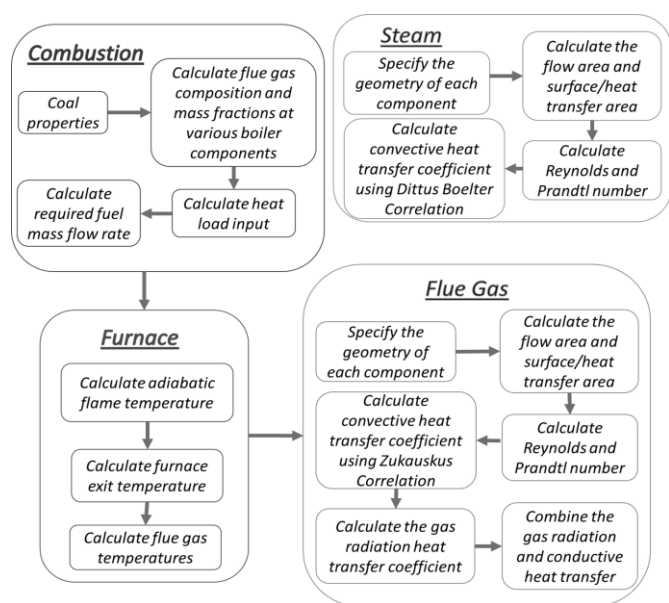


Figure 2: Flownex® methodology

3. QFT DESIGN OF A SINGLE ATTEMPERATOR-SUPERHEATER SUBSYSTEM

This section shows a tutorial style QFT design for a single SH stage, emulating the outer loop design in the conventional approach to superheater temperature control. This design provides a performance benchmark for evaluating the valve position control scheme in Section 4. Conventionally, a cascade design is used with a higher bandwidth inner loop around the attemperator to SH inlet temperature (regulating out valve and process uncertainty), with an outer loop to control the SH outlet temperature. The outer loop bandwidth is constrained by distributed parameter effects and valve rate limits.

Boiler Master Control

Boiler master control refers to the primary load demand signal interface between the turbine and boiler control. The boiler should be able to deliver the correct steam conditions according to the load demand. The two main outputs from the

boiler master control are the master air/fuel and the master feedwater setpoint. The master air/fuel is a common setpoint for boiler firing. Master feedwater is the common setpoint for the boiler feed pump controllers. The master fuel and master feedwater determine the mass flow and temperature setpoints of air-to-fuel ratio and feedwater required to produce the set megawatt (MW) load demand.

3.1. Robust Control

The presence of uncertainty in a model challenges the design as it is required to meet control specifications for every plant condition within the uncertainty range, not just a single plant with fixed parameters. Model uncertainty is generally a consequence of unknown dynamics, inaccuracies in parameter estimation, changes in operating point, fouling conditions, errors in sensors and actuators, system non-linearities and plant disturbance input. According to Borghesani, C., et al. (2003), one of the general control methodologies for dealing with the effects of uncertainty is Robust Control, as it uses a single fixed controller to design the “worst case” approach of a plant with uncertainty. QFT is a robust control technique that uses integrated theory to emphasizes the use of feedback design for computing parameters for a controller while satisfying closed loop performance specifications. It can deal with various performance specifications such as stability, disturbance rejection, reference tracking and noise rejection simultaneously. The main role of the controller is to reduce the effect of the uncertainties to an acceptable level. A Nichols chart is used to loop shape the frequency response according to the defined specifications.

Robust controllers were designed for attemperators 2 and 3 to maintain the main steam temperature at 540 °C. Figure 3 illustrates a one-degree-of-freedom closed loop system as using feedback allows for the desired output behaviour of the system to be achieved. In Figure 3, $P(s)$ is the uncertain plant (including actuator dynamics), $G(s)$ is the closed loop controller and $H(s)$ represents the dynamics of the sensor (typically, there will be some thermal inertia in measuring steam temperature due to the of the dynamics of the thermal well the sensor is in). The objective is to design a controller for $G(s)$ to ensure the output $Y(s)$ accurately tracks the input/reference demand $R(s)$ while rejecting the disturbance $D(s)$. The overall system transfer function from commanded temperature to output is,

$$\frac{Y(s)}{R(s)} = \frac{G(s)P(s)}{1 + G(s)H(s)P(s)} \quad (8)$$

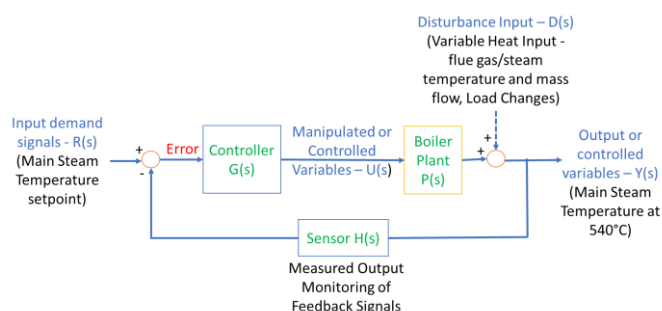


Figure 3: Feedback control system

3.2. A conventional single loop PI controller design

This section describes the design of a SISO PI controller using QFT methodology. Data, such as valve positions and temperatures, were extracted through a number of simulations using the developed Flownex® model which initiated the QFT process.

3.2.1. Plant models and uncertainty

The QFT design process began by defining the plant or system. In order to understand the potential and limitations of a system, an extensive model of plant dynamics is required in order to design a reliable control system to meet the specifications. The simulated data from Flownex® was modelled for the defined MCRs by changing the Attemperator 3 valve position and monitoring the dynamic effects on the input and output temperatures of the final superheater. This data was then exported to MATLAB® to identify the transfer functions for each dataset using the System Identification Toolbox. These open loop transfer functions define the plant models with uncertainty. A total of 6 disturbances to the system were simulated with the change in Attemperator 3 valve position defined as the input and the corresponding change in output temperature defined as the output. For a practical plant design, other operating conditions would need to be added to the plant set to capture the uncertainty envelope of the plant. The following equations (3 out of 6 data simulations) are the second order transfer functions modelled using system identification for a 10% increase in valve position for the various loads. (Other simulation scenarios include a 10% decrease in valve position vs output temperature):

$$P_{100}(s) = \frac{0.0071s - 0.0028}{s^2 + 0.1292s + 0.0048} \quad (9)$$

$$P_{97}(s) = \frac{0.0073s - 0.0028}{s^2 + 0.125s + 0.0045} \quad (10)$$

$$P_{70}(s) = \frac{0.0092s - 0.0021}{s^2 + 0.0923s + 0.0026} \quad (11)$$

Note that the identified models have non-minimum phase behaviour, and this is the result of trying to find a finite order linear model for the underlying distributed parameter system. The non-minimum phase behaviour will impose technical limits on the feedback bandwidth and input limitations also impose practical performance limits on the control design. (The system is reverse acting as increasing valve command reduces the temperature.) The above system identification results for measured responses with a worst-case root mean square error of 0.04 °C for P_{100} and 0.07 °C for P_{70} .

3.2.2. Nominal plant

In QFT design, the *nominal* plant $P_o(j\omega)$ is an arbitrary, fixed plant within the model uncertainty. Any plant can be selected as a handle for the subsequent design of the nominal open loop frequency response $L_o(j\omega) = P_o(j\omega) \cdot G(j\omega)$. The nominal plant chosen for this design $P_o(j\omega) = P_{97}(j\omega)$.

3.2.3. Templates

Plant templates are derived from the magnitude and phase plot of the parametrically uncertain plant set of transfer functions $P(j\omega)$ projected onto the Nichols chart. They characterise the plant parameter uncertainty region which is required for calculating the bounds at each discrete design frequency. Prior to obtaining the templates, the array of design frequencies for each bound is selected from inspection of the bode plot for each plant within the uncertainty. With $s = j\omega$ substituted into Equations (9) - (11), the selected low pass design frequencies to adequately cover the system's bandwidth are defined from Figure 4:

$\omega = [0.001, 0.01, 0.02, 0.03, 0.04, 0.06, 0.08, 0.1]$, resulting in 8 uncertain templates. The uncertainty region is marked with transparent lines, one on either side of the nominal model curve with the same colour as the curve. The plant templates modelled illustrates the set of points at each frequency, including the uncertainties. At low frequencies, the templates form a vertical line and become more spaced out at larger frequencies.

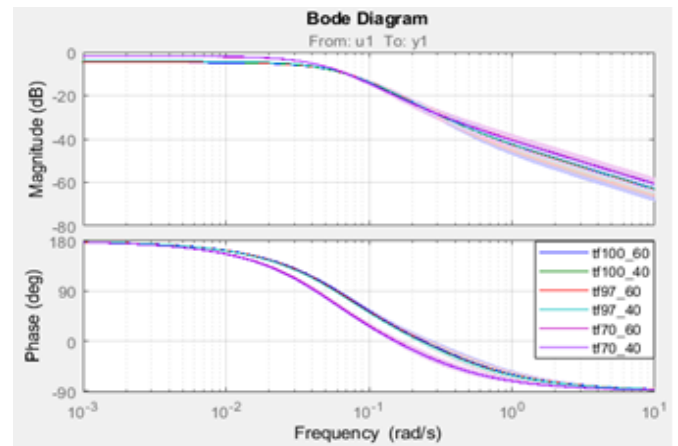


Figure 4: Magnitude (dB) and phase Bode plot showing confidence region for all plant sets

3.2.4. Specifications and bounds

If there are tracking specifications, these could be above and below bounds on the magnitude of (1) or tracking error bounds compared to model behaviour. For the purpose of illustration here, we are only considering regulation via bounds on the closed loop sensitivity (Garcia-Sanz, 2017):

(We are taking a short-cut to PI and PID design that would be quite typical in practice – we have defined a robust stability margin and maximized the low-frequency performance (including steady state error) and designed a low order controller within this constraint. More detailed control specifications can be accommodated easily.)

$$\text{zero steady state error} \quad (12)$$

$$\left| \frac{1}{1 + G(j\omega)P(j\omega)H(j\omega)} \right| \leq -20\text{dB}, \quad \omega \leq 0.001\text{rad/s} \quad (13)$$

$$\left| \frac{1}{1+G(j\omega)P(j\omega)H(j\omega)} \right| \leq 6\text{dB}, \forall \omega \quad (14)$$

The robust stability specification (14), $|1/(1+L)| \leq \gamma$ ensures gain margin, $g_m \geq \gamma/(1-\gamma) = 6\text{dB}$ and phase margin, $\phi_m \geq 2 \arcsin(1/(2\gamma)) = 29\text{deg}$.

The bounds provide the magnitude and phase constraints in which the closed loop system lie outside the bounds such that the desired process performance specifications are attained. It can be noted that there is a bound $B_k(\omega_i)$ for each frequency defined by ω and for each performance specification.

3.2.5. Loop shaping

The open loop robust stability bounds for all frequencies ω can be seen in Figure 5. Once the bounds are plotted on the Nichols chart, the controller $G(s)$ is designed by loop shaping using the nominal plant to meet its bounds. The nominal plant is only required for loop shaping since the various plant uncertainties and specifications have been integrated into the QFT bounds. It is therefore important that the nominal plant is loop shaped to the correct area for each frequency. Loop shaping involves frequency shaping of the nominal open loop frequency response such that the magnitude and phase of $L_o(j\omega)$ lies outside the nominal performance bounds for each ω . The solid line in Figure 5 denotes that L_o ‘stay above’ and a dashed line denotes ‘stay below’ the frequency of that bound. Horowitz explained that an optimum controller design is when $L_o(j\omega)$ is placed on top of each bound $B_k(\omega)$ for each frequency ω . The loop shaping methodology requires the addition of poles and zeros until the nominal loop lies near its bounds. The aim is to achieve the minimum possible controller magnitude (cost of feedback) at each frequency. The controller designed for this plant is shown in Figure 5. An integrator was added to accommodate for zero steady state error for step reference input and the gain was tuned to meet the low frequency bound at $\omega = 0.001\text{rads/s}$.

The loop shaping resulted in a PI controller which is represented below in standard form, where K_p is the proportional gain term and T_i is the integral time constant:

$$G_{\text{siso_att3}}(s) = K_p \cdot \left(1 + \frac{1}{T_i \cdot s} \right) = -0.65 \cdot \left(1 + \frac{1}{26.93s} \right) \quad (15)$$

Figure 6 shows the bode plot for systems L_o , $1/(1+L_o)$ and $L_o/(1+L_o)$, with the corresponding gain and phase margins for each system at its respective crossover frequency.

A similar approach was used to design a SISO PI controller for the attenuator 2 valve:

$$G_{\text{siso_att2}}(s) = K_p \cdot \left(1 + \frac{1}{T_i \cdot s} \right) = -0.58 \cdot \left(1 + \frac{1}{24.2s} \right) \quad (16)$$

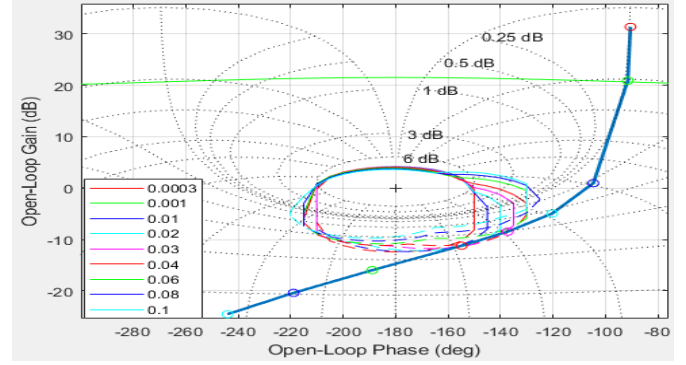


Figure 5: Loop shaping for $L_o(s)$

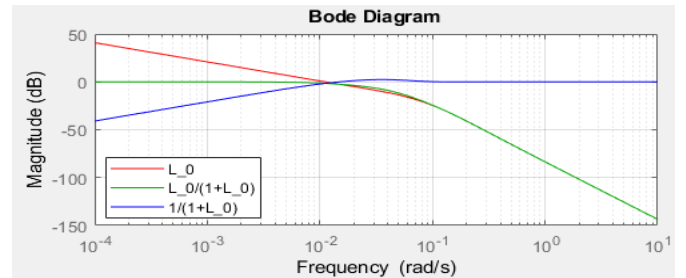


Figure 6: PI controller design bode plot

4. VALVE POSITION CONTROL

This section details a valve position controller design which uses a similar approach to the SISO PI controller designed using the QFT technique. Shinskey (1978) has introduced the concept of valve position control for energy and efficiency optimisation in process control. It can be noted from Figure 7 that a VPC consists of two controllers, where $G_3(s)$ is the faster response controller that controls the process output variable $T_{3,out}$, and $G_2(s)$ ‘‘mid-ranges’’ $G_3(s)$ while controlling the valve position $U_2(s)$. In the case of the power plant, we set the reference valve position to 10% so that there is still control authority in both directions but spray water injection higher up in the flue gas pass is preferred for the purpose of higher thermal efficiency. The control objective is to manipulate both controller variables upon a disturbance, where the controlled variable, $U_2(s)$ of $G_2(s)$, gradually manipulates the $G_3(s)$ control variable, $U_3(s)$, to its desired steady state value (10%) to accommodate for the changes in dynamics. Figure 7 represents the VPC system architecture used to test the technique in Flownex®.

Equation (17) summarises the normal transfer function from input control to output where the indices correspond to the input labels. P_{22} manipulates $U_2(s)$ which influences the change of steam temperatures T_2 . Similarly, P_{33} manipulates $U_3(s)$ which influences steam temperature T_3 . However, P_{23} and P_{32} are very low pass behaviour, where $U_2(s)$ has a slow coupling effect on T_3 through steam flow and $U_3(s)$ a slow coupling effect on T_2 through the change in flue gas temperatures entering RH2 and SH2.

$$\begin{pmatrix} T_2 \\ T_3 \end{pmatrix} = \begin{pmatrix} P_{22} & P_{23} \\ P_{32} & P_{33} \end{pmatrix} \begin{pmatrix} U_2 \\ U_3 \end{pmatrix} \quad (17)$$

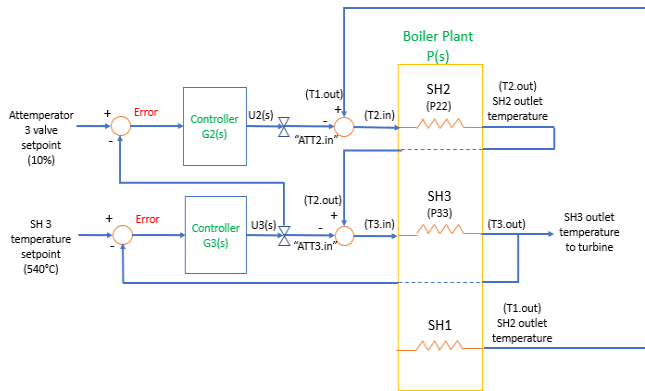


Figure 7: Valve position control system

Using the QFT loop shaping method described in Section 3.3 above, the VPC controllers were designed as follows:

$$G_{VPC_att2}(s) = K_p \cdot \left(1 + \frac{1}{T_i \cdot s}\right) = -0.712 \cdot \left(1 + \frac{1}{44.9s}\right) \quad (18)$$

$$G_{VPC_att3}(s) = K_p \cdot \left(1 + \frac{1}{T_i \cdot s}\right) = -0.65 \cdot \left(1 + \frac{1}{26.93s}\right) \quad (19)$$

It is noted that the VPC and SISO controllers for attemperator 3 valve are comparable as expressed in equation (19) and equation (15). However, the controllers designed for attemperator 2 valve, the VPC controller (equation (18)) is slower than the SISO controller (equation (16)) due to the greater lag from $U_2(s)$ to $T_{3.out}$, as explained using equation (17) above.

5. RESULTS

Figure 8 shows the Flownex® model which was simulated for a 20 °C increase in flue gas temperature (such a step is not realistic in the practical system) at 100% MCR operating conditions with a valve position controller. It can be noted from this figure that the purple line is the signal for $U_2(s)$ which settles at ~57 %, the red line is the $U_3(s)$ signal which settles at 10% (as designed) and the blue line is the final main steam temperature which is controlled to settle at 540 °C, as per setpoint.

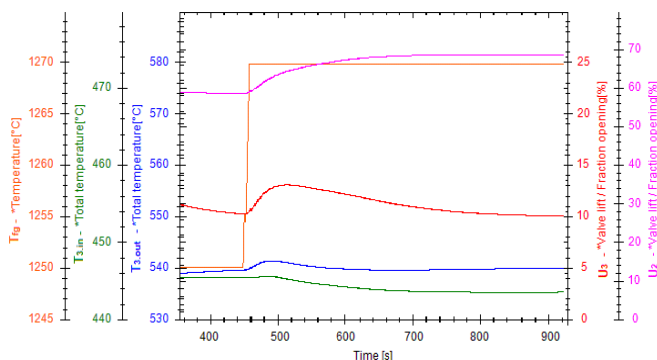


Figure 8: Flownex® simulation using VPC

Table 2 compares the steady state heat uptake per superheater pass for the VPC and SISO PI controller schemes. Notice that the VPC is 1 % more efficient compared to the SISO PI

controller application by the simple expedient of spraying the required amount of attemperator water as high up the flue gas pass as possible, thereby increasing the total heat uptake (by approximately 4 MW in this example).

Table 2: Heat uptake (MW) for 100% and 70% MCR

	100% MCR		70% MCR	
	VPC	SISO	VPC	SISO
SH2	78.4	74.1	50.8	47.0
SH3	154.2	154.2	111.6	111.6
SH1	60.1	60.1	45.5	45.5

6. CONCLUSIONS

Coal fired power plant are non-linear as a result of underlying nonlinearities in the dynamic model, changing operating conditions and parameters. It is not possible to achieve effective robust control when the boiler is modelled using a single operating point and is therefore essential that the controller design methodology accounts for disturbances in conjunction with the uncertain boiler model. This paper compares the QFT design of SISO PI controllers and valve position controllers to investigate the improvement over the current attemperator control design.

7. REFERENCES

- Borghesani, C., Chait, Y and Yaniv, O. (2003). *The QFT Frequency Domain Control Design Toolbox For Use with MATLAB® user guide*. Terasoft.
- Garcia-Sanz, M. (2017) *Robust Control Engineering*. United States of America: CRC Press. ISBN 13: 978-1-138-03207-1
- Horowitz, I. (2001), Survey of quantitative feedback theory (QFT). *Int. J. Robust Nonlinear Control*, 11: 887-921. doi:10.1002/rnc.637
- M-Tech industrial. (2019), *Flownex Library Manual* (for Flownex® Software simulation version 8.9.1.3598), South Africa
- Molbak, T. and Mortensen, J.H. (2003). ‘Steam temperature control’, in Flynn, D. *Thermal Power Plant Simulation and Control*, United Kingdom: The Institute of Electrical Engineers. pg 131-160.
- Sanchez, L. A., Arroyo, F. G. and Villavicencio, R. A. (1995). *Dynamic matrix control of steam temperature in fossil power plants*, IFAC Proceedings Volumes. Elsevier, 28(26), pp. 275–280.
- Schlunder, E. U. (1983). *Heat exchanger design handbook*. Washington: Hemisphere Pub. Corp.
- Shinskey, F.G. (1988). *Process Control Systems*, United States of America: McGraw-Hill.
- Shinksey, F. G. et al. (2006) ‘Control Systems - Cascade Loops’, in Liptak, B. G. (ed.) *Process Control and Optimization*. United States of America: CRC Press, pp. 148–156. doi: 10.1007/978-1-4899-4467-2_7.
- Spliethoff H., Klefenz, G., Nicolai, W., and Trautmann. G. (1986). *Experience and results with the state controller for the live steam temperature control of a 2250 T/h steam generator*, BWK, vol. 38, no. 10, pp. 441-447.
- Zhang, Y., Li, Q. & Zhou, H., (2016). *Theory and calculation of heat transfer in furnaces*. London: Elsevier.